geosciences

MDPI

Review

Excessive Southwest Greenland Ice Sheet Melting Between 4.4 and 3.2 ka BP Documented by Fjord Sediments: Implications for N-Atlantic Ocean Circulation and AMOC

Antoon Kuijpers [1,*] and Marit-Solveig Seidenkrantz [2]

[1] Geological Survey of Denmark and Greenland, Øster Voldgade 10, 1350 Copenhagen K, Denmark
[2] Department of Geoscience, Aarhus University, Høegh-Guldbergs Gade 2, 8000 Aarhus C, Denmark; mss@geo.au.dk
* Correspondence: aku@geus.dk

Abstract

Greenland Ice Sheet (GrIS) melting occurred during the later part of the Holocene Thermal Maximum (HTM) with a well-documented significant GrIS retreat between 7 and 3 ka. However, less is known about the immediate melt water impact on Greenland fjord hydrography and more distant ocean circulation. A compilation of published sediment records from southwest Greenland fjords and Disko Bay, West Greenland, demonstrates marked local erosional events and deposition of extensive (silty) melt water sediments within the period 4.4 to 3.2 ka BP. The termination of fjord perturbation in this region is dated at c. 3.2 ka and closely corresponds to the reported timing of minimum GrIS extent. As an ocean response, an increased freshening and enhanced melt water transport by the Labrador Current (LC) between 4.4 and 4.0 ka are concluded to signal the most prominent melt water discharge events in the southwest Greenland fjords. The latter melt water pulses were coeval with a marked warming episode and negative surface mass balance peak recorded in ice cores. As suggested by modelling and paleo-oceanographic records from the North Atlantic subpolar gyre, temporarily enhanced GrIS melting and increased LC freshwater release into the North Atlantic around 4.2 ka may have led to destabilization of the AMOC. The GrIS melt water surges associated with an anomalous atmospheric (Greenland blocking) regime are proposed to reflect a regional climate anomaly related to the so-called '4.2 ka BP event'.

Keywords: Greenland; Holocene Thermal Maximum; ice sheet melting; sediments; fjord and ocean circulation; AMOC

Check for updates

Academic Editor: Evgeny Chuvilin

Received: 20 July 2026
Revised: 1 September 2026
Accepted: 6 September 2026
Published: 15 September 2026

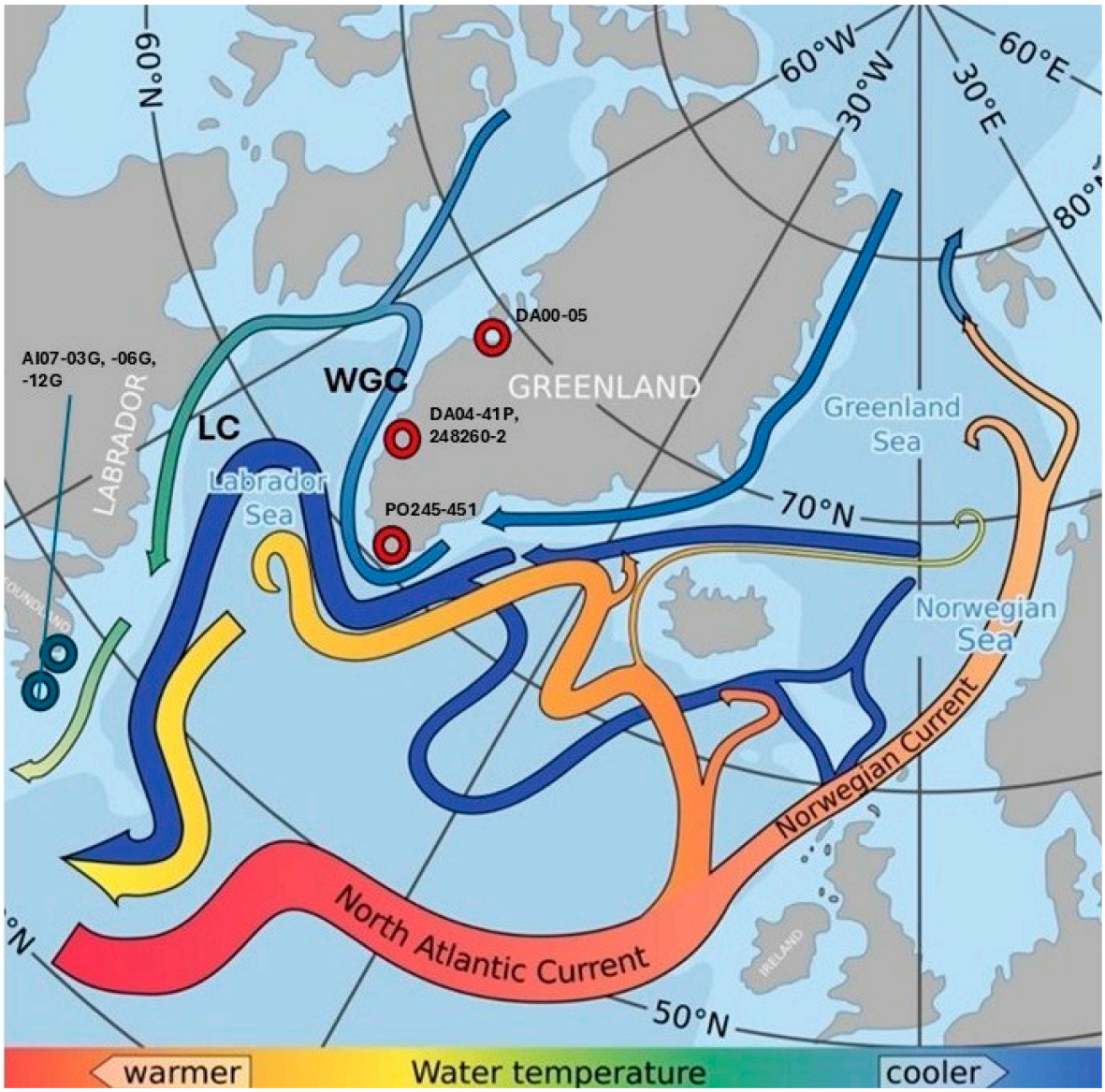
Copyright: © 2026 by the authors. Licensee MDPI, Basel, Switzerland. This article is an open access article distributed under the terms and conditions of the Creative Commons Attribution (CC BY) license.

1. Introduction

An early-to mid-Holocene Thermal Maximum (HTM) has been documented in many high-latitude and Arctic climatic records of the Northern Hemisphere [1]. Lake records in Greenland indicate that atmospheric summer temperatures locally were 2–4 °C higher than observed today, with a particularly persistent warming in West Greenland occurring between 6 and 4 ka [2]. The warm conditions led to excessive circum-Greenland Ice Sheet (GrIS) melting and thinning [3], with the ice sheet margin retreating behind present-day extent [4,5]. The minimum extent of the southwest GrIS was reached near the end of the HTM between 5 and 3 ka [6,7], when the ice sheet again started to gradually expand due to the subsequent onset of Neoglacial cooling. Apart from higher temperatures, the climate regime during the HTM was characterized by increased windiness and precipitation [3,8,9].

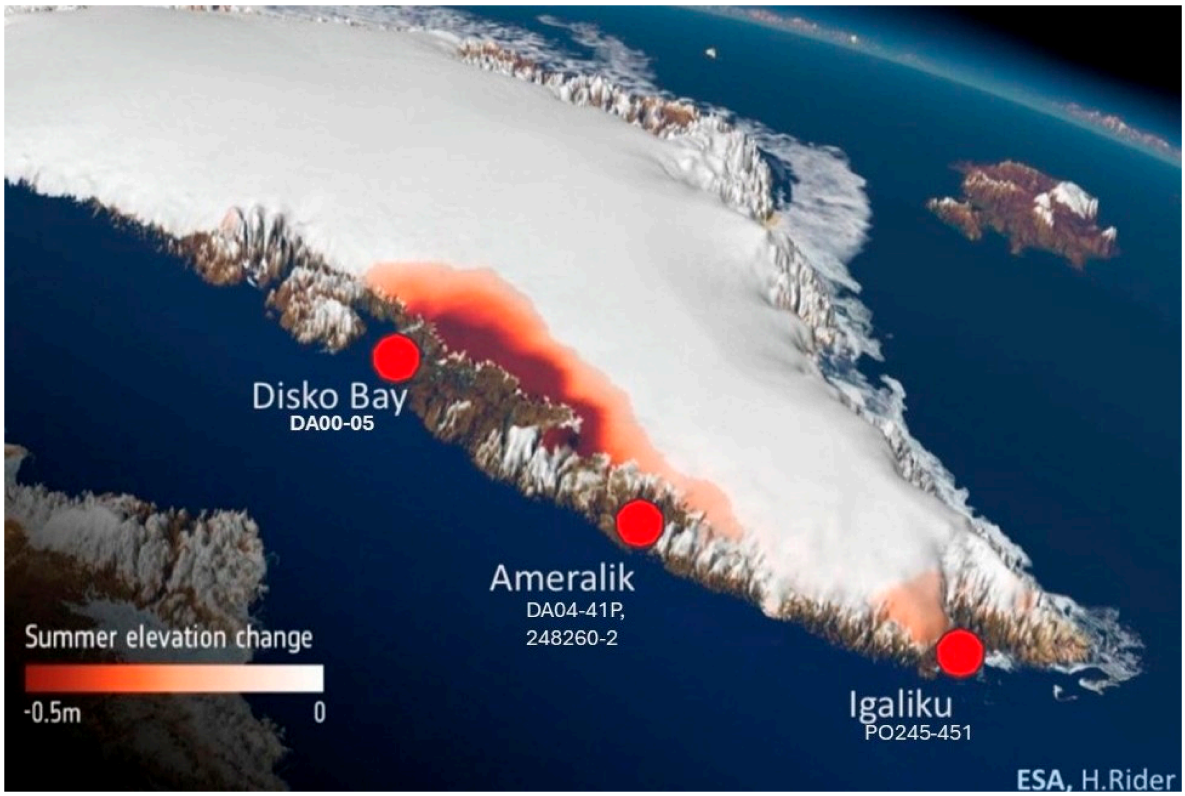
This variety of records thus clearly document warmer-than-present climate conditions and reduced GrIS extent in SW Greenland during the mid-Holocene.

A recent study [10] illustrated the impact of glacier retreat after the last glaciation on fjord bedforms in the Nuup Kangerlua (Godthåbsfjorden) region, where the Ameralik Fjord is one of the study areas (Figure 1). However, the direct impact of widespread ice sheet melting on fjord hydrographical circulation and ocean dynamics is still poorly understood. This is the case for the impact of the late HTM ice retreat in particular. The effect of more limited, regional glacier retreat on fjord environments and ocean circulation is even less known. Presently, according to a number of model simulations the ongoing GrIS melting would significantly weaken the Atlantic Meridional Overturning Circulation (AMOC, Figure 1a). It is, however, highly debated whether this AMOC weakening would lead to a complete collapse [11,12].



(**a**)

Figure 1. *Cont.*



(**b**)

Figure 1. (**a**) North Atlantic circulation (base map:https://en.wikipedia.org) with the North Atlantic Current transporting warm, saline surface waters polewards, where in the Greenland and Labrador Sea cooling and evaporation lead to the formation of cold, dense water masses that flow south at depth. These sink water processes are crucial in maintaining a surface-to-deep water mass transfer known as the Atlantic Meridional Overturning Circulation (AMOC). The areas where Greenland fjord sediments reveal excessive glacier melting 4400 to 3200 years ago are indicated by open, red dots, whereas seabed sediment sites in coastal waters off Newfoundland with records of Labrador Current hydrographic changes are marked by open, blue dots. Key sediment core IDs (see Table 1) are also indicated. LC = Labrador Current; WGC = West Greenland Current; (**b**) Southwest Greenland areas where particularly strong ice sheet melting had occurred in 2020 (European Space Agency, ESA) and 2021 (National Snow and Ice Data Center, NSIDC). The red dots indicate the areas where fjord sediment cores document strong glacier melting 4400 to 3200 years ago.

Table 1. Summary of key sites with sediment core information and respective publications representing the framework of our review study. The sediment coring sites in coastal waters off eastern New-foundland are located in several embayments ([1] = Bonavista Bay; [2] = Placentia Bay; [3] = Trinity Bay).

Author & Ref. No.	Core ID & Area	Latitude	Longitude	Water Depth (m)	Core Length (m) with Number of AMS ^{14}C Datings
Lloyd et al. [13]	DA00-05 mouth of Kangersuneq fjord, Disko Bay	68°42′92″ N	51°06′42″ W	335	10.48 m (7)
Ren et al. [14]	DA04-41P Ameralik	64°05.388′ N	51°15.038′ W	744	8.58 m (12)
Møller et al. [15], Seidenkrantz et al. [16]	248260-2 Ameralik	64° 05.433′ N	51°15.530′ W	674	3.48 m (5)

Table 1. *Cont.*

Author & Ref. No.	Core ID & Area	Latitude	Longitude	Water Depth (m)	Core Length (m) with Number of AMS^{14}C Datings
Lassen et al. [17]	PO245-451 Igaliku	60°41.96′ N	46°02.00′ W	304	3.51 m (9)
Solignac et al. [18]	AI07-03G Newfoundland [1]	48°44.321′ N	53°29.181′ W	329	4.72 m (7)
Solignac et al. [18]	AI07-12G Newfoundland [2]	47°08.204′ N	54°33.182′ W	230	4.75 m (4)
Orme et al. [19]	AI07-06G Newfoundland [3]	47°85′ N	53°58′ W	511	4.31 m (9)

Our review study will therefore focus on the impact of late HTM ice sheet melting on the hydrography of three southwest Greenland fjords and possible implications for more distant ocean circulation, especially AMOC. We choose this study region as recent satellite data have shown the ice sheet in the area to be especially sensitive to modern warming with strong ice sheet melting occurring in recent years (Figure 1b). We compare sediment records from three southwest Greenland fjord systems (for study areas, see Figure 1) that are all located within one of these actual melting sectors of the GrIS. This is supplied by sub-bottom information from an adjacent near-coastal site. In addition, we compare these data with marine sediment records from coastal waters off eastern Newfoundland, where the Labrador Current (LC, Figure 1a) carries melt water from West Greenland and the northeast Canadian archipelago towards the subpolar gyre of the North Atlantic Ocean with direct impact on the AMOC [20,21].

2. Material and Methods

The material used for this review study primarily consists of eight publications listed in Table 1, which shows information on key sediment core location, sediment core length, and number of AMS^{14}C datings applied at each of these cores. Each of these publications provides detailed information on the chronology and various analytical methods employed. The many AMS^{14}C sediment datings (Table 1) in these cores with only a few exceptions reveal a dating error range of generally less than 100 years. Within this context it is noteworthy that the reconstruction of a regional ocean–atmosphere–cryosphere regime discussed below yields a very coherent picture with regard to the chronology of the various environmental records, despite the fact that these are based on widely different dating methods (AMS^{14}C dates, ice core chronology, and geological field observations). In addition to dating, in all sediment cores a multi-proxy parameter approach was applied which included micropaleontological components (foraminiferal fauna, dinoflagellates cyst assemblages, diatom flora), XRF multi-element analysis, and grain-size measurements including sediment modelling. For a detailed methods description we refer to the original publications. It must be noted, however, that the selected multi-proxy parameters vary from core to core, with one exception, which is the analysis of the foraminiferal fauna. Increasing knowledge of the effect of GrIS melting on AMOC behaviour and its possible weakening under a further climate warming has been crucial for our decision to make a compilation of this archive data set available for public information.

3. Results

3.1. Holocene Hydrographic Records from Southwest Greenland Fjords

The three southwest Greenland fjords that are the focus of this review are all located in regions that have experienced particularly strong ice sheet melting in recent years (Figure 1b). The ocean circulation offshore is characterized here by the prevalence of the West Greenland Current (WGC, Figure 1a), which transports relatively warm and saline Atlantic water masses derived from the Irminger Sea towards the north [20], with its core between 200 and 600 m water depth [22]. This warm water plays a crucial role in subglacial melting of the southwest Greenland tide-water glaciers [23], and satellite images clearly illustrate the presence of melt water plumes at the mouth of several southwest Greenland fjords, being entrained in a northerly direction by the WGC (Figure 2). The uppermost WGC waters involved in this entrainment are colder and less saline than the underlying Atlantic-derived water mass [22] and originate from the melt water discharge from the GrIS mixed with low-salinity Polar water masses initially advected southward by the East Greenland Current [24]. For summarized information on the key sediment coring sites with respective publications that have been the framework of our study, refer to Table 1.

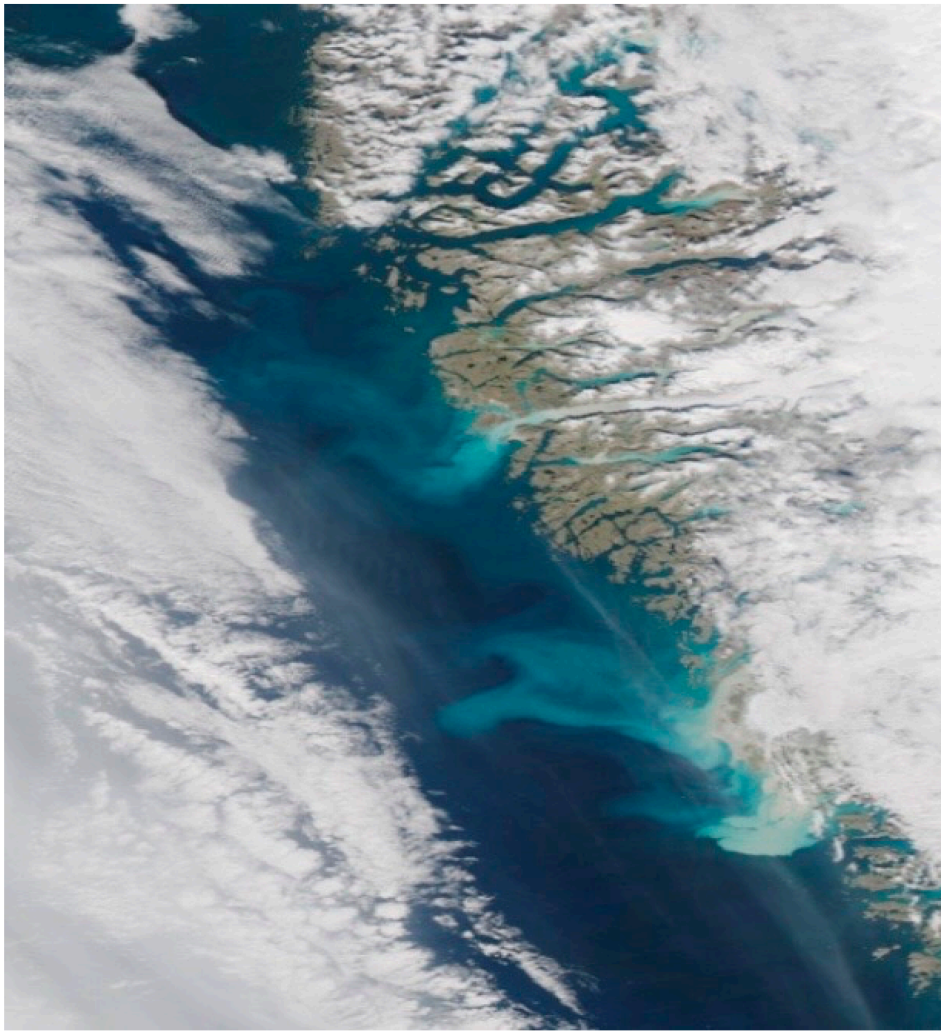


Figure 2. Satellite image (https://earthobservatory.nasa.gov/IOTD/view.php?id=84464, accessed on 20 May 2026)) showing large, sediment-rich melt water plumes exiting from West Greenland fjords being entrained to the north by the West Greenland Current.

In the Disko Bay area, i.e., the northern sector of the modern melting region (Figure 1b), a marine sediment core (DA00-05, see Table 1) was retrieved from the mouth of Kangersuneq fjord, exiting in the southeastern part of the bay [13]. At around 4.5 m core depth the Holocene depositional record from this site reveals a major ice-rafted-detritus (IRD) event documented by markedly increased silt and fine-sand fluxes dated between ca. 4.0 and 3.5 ka. According to benthic foraminiferal assemblage data of this core, the glacial surge coincided precisely with a period of significantly increased warm WGC inflow into Disko Bay. A high-resolution sub-bottom profile of the Disko Bay seabed (Figure 3) obtained about 7 km offshore of the latter coring site shows a transparent, virtually undisturbed upper acoustic unit indicative of regular Holocene sedimentation [25]. However, within the upper part of this Holocene unit, one single reflector is visible at 5–7 m below the seabed. The transparent unit of fine-grained Holocene sediments is known to consist of fast accumulated melt water deposits with sedimentation rates decreasing towards the late Holocene [26]. The acoustic stratigraphy displaying this single reflector at 5–7 m sub-bottom depth is concluded to illustrate a prominent glacial surge event with a silt–sandy IRD deposit on the Disko Bay shelf and based on a comparable depth, we suggest that the reflector is correlatable with the IRD layer in the fjord core DA00-05 [13]. This shows that this area of Disko Bay may have experienced a significant change in the marine environment in that late Holocene period. On the open shelf, not far south of Disko Bay, hydrographic conditions are also reported to have changed around 3.8 ka [27].

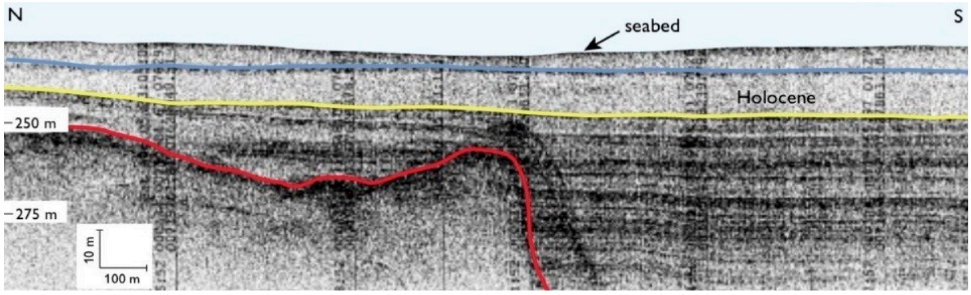


Figure 3. High-resolution (CHIRP) sediment sub-bottom record from the southeastern part of Disko Bay [17–23] (p. 3) showing an upper, Holocene transparent unit (above the yellow reflector) overlying laminated de-glacial sediments (between red and yellow lines). The red line shows the top of the acoustic base-ment. This upper Holocene unit above the yellow reflector displays one single internal (blue) re-flector situated 5–7 m below the seabed. The reflector is concluded to represent a prominent silt–sandy IRD deposit which has been found in a nearby 10.48 m long piston core (DA00-05) and dated between c. 4.0 and 3.5 ka [13] (p. 2).

In the present melting region further to the south, the Ameralik Fjord (see Figure 1b), which is part of the larger Nuup Kangerlua (Godthåbsfjord) fjord complex, is another area where several sediment records provide evidence of significant hydrographic perturbation and disturbance of regular sedimentation. In sediment core DA04-41P (see Table 1) a significant hiatus over the period 6.8 to 4.4 ka was found [14]. Another sediment core (248260-2, Table 1), located close by and near the mountainous north side of the fjord, displayed an interval of massive, silty melt water sediments deposited between 4.4 (core bottom) and 3.2 ka [15]. Modelling of the sediment grain size data from this interval confirmed that deposition can be ascribed to suspension settling processes from melt water plumes. At the same time foraminiferal benthic faunas from this core indicated that an otherwise persistent inflow of warm, saline Atlantic-derived water masses at depth weakened and became unstable after ca. 3.2 ka [16]. Furthermore, multi-proxy records from sediment cores taken at a water depth of 399 m in the innermost part of the Nuup

Kangerlua fjord complex confirm that higher-than-present Atlantic water influx prevailed at that site between 7 and 3 ka, with a peak of Atlantic water influence from 5 to 3 ka [28].

In southern Greenland, benthic foraminiferal data from a marine sediment core (PO245-451, Table 1) collected in the Igaliku fjord (Figure 1b) likewise reveals prevalence of Atlantic-derived water masses during the later part of the Holocene [17]. On this site, an interval with sandy and silty melt water sediments and a major hiatus separates late Holocene sediments deposited after 3.2 ka from an early Holocene (>7 ka) sediment sequence of mainly turbiditic origin.

3.2. Holocene Hydrographic Records from Coastal Waters off Eastern Newfoundland

Ocean circulation in coastal waters off eastern Newfoundland is characterized by the Labrador Current (LC, Figure 1a), which transports cold, low-salinity water masses southwards, including melt water from the GrIS and local ice caps in the Canadian archipelago [20,21] (p. 2). In this area sediment cores from sites in three different embayments (see Table 1) were investigated for Holocene variations in LC activity, salinity, and sea surface temperature (SST) [18,19]. The results of these studies demonstrate that the lowest SST values occurred in the period 5.7 to 4.0 ka and were associated with higher amounts of terrestrial elements and detrital carbonate. Moreover, a long-lasting minimum in salinity has been recorded in the period 4.5 to 4.0 ka.

4. Discussion

4.1. Greenland Fjord Water Perturbation Due to Enhanced Melt Water Discharge

The Holocene sediment records from the three fjord areas in Southwest Greenland all signal enhanced melt water discharge and a coeval deep inflow of Atlantic-derived (WGC) water masses during the late HTM. These conditions prevailed until the onset of gradual Neoglacial cooling finally affecting all areas after 3.2 ka. In these fjords that form the main melt water gateway between the GrIS and the open ocean, saline ocean waters interact directly with tide-water glaciers and outflowing GrIS melt water streams. In exchange with the Labrador Sea and Baffin Bay, Atlantic-derived, warm and saline water today flushes these deep fjords at subsurface depth [29]. Buoyant plumes of glacial melt water from tide-water glaciers and riverine runoff rich in suspended matter flow in the opposite direction towards the open sea (Figure 2). Increasing melt water fluxes lead to enhanced estuarine circulation, in turn favouring an increased inflow of Atlantic-derived water at depth. As illustrated in the satellite image of Figure 2, this circulation pattern is today responsible for entrainment and export of large amounts of suspended, fine-grained (silty) sediment towards the open ocean [30,31]. On the West Greenland shelf such deposits of terrestrial origin are recognizable owing to their elemental composition, which reveals here widespread deposition of suspended matter from melt water plumes during the early- and mid-Holocene [32]. The acoustic reflector in the upper part of the Holocene unit from Disko Bay (Figure 3) may illustrate such enhanced fjord-to-shelf transport of more proximal, glacially derived sediment, in this case having occurred in the late Holocene, i.e., 4.0 to 3.5 ka [13] (p. 2).

With regard to the bathymetric setting of the sediment cores involved in this study, it is important to note that all coring sites have a water depth within the depth stratum of warmer, Atlantic-derived WGC shelf water masses. In the 75 km long, WSW-ENE trending Ameralik Fjord, despite its deep basins, the bottom water masses are, however, isolated from a direct inflow of these Atlantic-derived subsurface masses due the presence of a shallow (110 m) sill at its entrance. Still, a strong tidal-induced mixing at the outer sill enables a dense inflow of relatively saline water masses leading to deep water renewal, particularly during the winter [33]. In contrast to the other fjords of Nuup Kangerlua,

there are presently no marine-terminating glaciers in the Ameralik Fjord, which implies that subglacial freshwater discharge does not occur here. The fjord receives, however, a significant freshwater flux of melt water throughout the year through riverine discharge of freshwater at the head of the fjord. We suggest here that the sediment hiatus in the deep basin of the Ameralik Fjord, spanning the period 6.8–4.4 ka [14] (p. 3), may be attributed to a significant erosional event as lithological and geochemical evidence of a sediment 'hardground' is lacking, which excludes a longer period of non-deposition. Erosion due to mass flow or turbidity flow action is also unlikely, as the XRF element data do not show any sign of allochthonous sediment influx. We propose that intensified mixing processes and temporarily enhanced deep water inflow flushed the fjord immediately prior to 4.4 ka. This is supported by the fact that mid-Holocene sediments underlying this hiatus display a trend of increasing silt admixture and cooling indicative of higher bottom water hydrodynamic energy promoted by enhanced estuarine circulation and mixing processes at the sill. Such increased deepwater renewal can be explained by strongly enhanced export of low-density (melt) water at the surface. In addition, increased WGC flow activity over the shelf after 5 ka [32] (p. 4) may have further contributed to the enhanced mixing processes at the outer sill of the Ameralik fjord. The sediment core records from inner Nuup Kangerlua also reveal exceptional influence of Atlantic-derived water masses having occurred in particular after 5 ka [28] (p. 3). This is further supported by analyses of reworked bivalve shells from coastal sites further to the north, showing optimum ocean conditions between 5 and 3 ka [7] (p. 1). Both the timings of excessive melt water discharge in Disko Bay (c. 4.0 ka) and the Ameralik Fjord (c. 4.4 ka) correspond to an episode of positive temperature anomalies in Greenland ice cores and on Ellesmere Island, Arctic Canada [34,35]. This warming around 4.2 ka is also reflected in a prominent negative anomaly in the GrIS mass balance [36]. A remarkable increase of mercury accumulation found in the Greenland EGRIP ice core has been dated at 4.3 to 3.8 ka [37]. Recent measurements of ocean-to-atmosphere fluxes of mercury could demonstrate that riverine-influenced coastal waters display markedly higher mercury fluxes than open ocean surface waters farther away from the coast [38]. We thus tentatively propose that the reported mercury anomaly originates from increased mercury fluxes released from extensive melt water plumes in Greenland coastal waters.

Sediment core 248260-2 (Table 1) from the Ameralik Fjord was collected close to the northern side of the fjord [22] (p. 2) and has a basal date of c. 4.4 ka. The top of the thick, massive silty melt water deposit representing the lower unit of the core has an age dated at 3.2 ka. We observe here a transition to mainly clay-sized sediments indicating a well-defined ceasing of melt water flow. However, in the deep basin core nearby (DA04-41P) the sediment facies of the interval 4.4 to 3.2 ka do not show any sign of massive silt deposition such as observed in the core taken close to the north side of the fjord. A possible explanation could be a strong estuarine flow regime with Ekman-transport forcing the outflowing sediment-loaded melt water to be concentrated along the northern side of the fjord. One could further speculate whether the landscape with moraines and smaller valleys on the north side of the fjord [39] provided an environment from which local glaciers had contributed with silt-loaded melt water with proximal perturbation of the outflowing melt water stream along the northern fjord side. On the shelf outside the Ameralik fjord, lower surface-water salinities during the late HTM show that melt water release from Greenland was sufficiently strong enough to affect the WGC regime of the open shelf sea [40].

The sediment record from the Igaliku Fjord in southern Greenland [17] (p. 3) shows that environmental conditions characterized by frequent turbidite deposition in the early-Holocene were followed by a period of high-energy bottom water dynamics and melt water flow which lasted until c. 3.2 ka. The sandy and silty sediment unit marking this period includes a hiatus as well. The age of this possible hiatus could, however, not be determined

with confidence. The foraminiferal data also confirm that during most of the Holocene at this site Atlantic-derived water masses had prevailed in the deeper parts of the fjord. The termination of excessive melt water flow in this fjord dated at 3.2 ka corresponds notably well with the start of regrowth of local glaciers in South Greenland after 3.0 ka [41].

4.2. Labrador Current Melt Water Export and Possible AMOC Instability

In the North Atlantic Ocean the AMOC surface branch is formed by the poleward transport of warm, saline waters by the Gulfstream-North Atlantic Current system (Figure 1a) where at higher latitude the Greenland and Labrador Sea cooling and evaporation lead to deep convection. These processes result in the formation of dense and cold water masses that flow south at depth. The direct impact of this Atlantic circulation system on climate is immense, which particularly applies to the European climate. As mentioned before, it is a matter of international debate whether increasing melt water release from Greenland in the near-future may lead to an AMOC disruption. Estimates of the impact of recent freshwater fluxes from Greenland on deep convection in the Labrador Sea suggest the possibility of an AMOC weakening [42]. The reported seabed sediment records from coastal waters off eastern Newfoundland [18,19] (p. 3) show lowered SST values in the period 5.7 to 4.0 ka and a long-lasting minimum in salinity between 4.5 and 4.0 ka. Sediments from the latter period are further characterized by higher amounts of terrestrial elements and detrital carbonate, the latter component presumably originating from the surroundings of Ellesmere Island. This data set clearly signals enhanced LC advection of low-salinity (melt) water masses from Greenland and to a minor extent presumably also from local icecaps in northeastern Canada (e.g., Ellesmere Island). The timing of these LC anomalies excludes other melt water sources of any significance. The glacial North-American Laurentide Ice Sheet had completely disappeared a few millennia earlier. This low-salinity (melt)water mass transport by the LC along the Canadian coast is part of a large-scale cyclonic circulation pattern including the northward transport of Atlantic-derived warmer and saline water by the WGC along the coast of West Greenland (Figure 1a).

Recently, enhanced northward transport of heat by the WGC and strong GrIS melting could be linked to an atmospheric circulation pattern characterized by extreme Greenland blocking and a shift in regional cyclone tracks [43]. In analogue, a relatively frequent occurrence of such an atmospheric circulation regime may have led to increased northward advection of Atlantic-derived water masses by the WGC between 5 and 3 ka, reaching a peak in the period 4.4 to 4.0 ka. As discussed above, this is suggested by prominent melt water pulses indicated by the sediment records from Ameralik Fjord (4.4 ka) and Disko Bay (4.0 ka) and anomalies occurring in WGC and LC hydrography. A puzzling and temporarily accelerated sea level rise between 4.5 and 3.8 ka at the Nova Scotian coast [44] also here confirms changes in the coastal hydrography of the LC. The latter authors tentatively propose that this temporary sea level rise may be attributed to an enhanced LC export of melt water released from the Arctic. An overview of GrIS excessive melting and concurrent ocean anomaly patterns is presented in Figure 4. An atmospheric circulation regime with Greenland blocking and shifted cyclone tracks [43] points to a changed wind regime which could have been favourable for initiating a higher sea level stand at the Nova Scotian coast. Within this context we refer to a recent study [45] describing a highly complex relationship between summer warming, freshening and cessation of Labrador Sea deep convection leading to a marked sea level rise. Thus, apart from freshwater influxes due to southwest Greenland melting, the regional atmospheric circulation regime is a crucial factor in controlling deep convection in the Labrador Sea [46]. In particular in summer these atmospheric conditions also are linked to the atmospheric circulation pattern with an anomalous anticyclone over Greenland, which appears to respond to large-scale Arctic warming and

a reduced North American Snow cover [47]. About 4200 years ago such conditions did indeed occur in continental North America, and also at that time severe centennial-scale drought occurred [48]. Strong Greenland blocking in that period is further indicated by (exotic) pollen assemblages from Newfoundland and surrounding waters [49,50] pointing to warm spring/summer conditions favoured by frequent occurrence of southerly winds in association with an anticyclone ridge over (southern) Greenland. It is thus evident that increased LC freshwater transport is not the only factor controlling deep convection in the Labrador Sea.



Figure 4. Overview map of Greenland Ice Sheet excessive melting and concurrent ocean anomaly patterns 4.4 to 3.2 ka BP. It is important to note that Labrador Sea deep convection is controlled by complex, large-scale air–sea exchange process patterns, which include, among others, freshwater input (dark blue arrows) from Greenland and other Arctic regions [45,46]. WGC = West Greenland Current (light blue arrow pointing north); LC = Labrador Current (light blue arrows pointing south). Base map from https://www.Wikimedia.org.

Within this context it is important to underline that this period around 4.2 ka represents a climate anomaly that is not only restricted to Greenland and adjacent regions, as it has been documented in many parts of the world and is known as the so-called 4.2 ka BP event [51,52]. In analogue to studies pointing to a possible future AMOC weakening [31] (p. 5), enhanced LC freshwater transport associated with prominent GrIS melting pulses in the period 4.4–4.0 ka may have led to a temporary AMOC destabilization. Such a temporary disruption of the AMOC around 4.2 ka has been confirmed in modelling experiments [53], and is also suggested by paleo-oceanographic studies. These have shown, amongst others, a North Atlantic SST pattern indicative of a weakening of the subpolar gyre circulation around 4.2 ka [54]. These changes included a marked transition shortly after c. 4.0 ka from fresher, more nutrient-rich water masses circulating in the subpolar gyre to more saline surface water conditions as recorded off NW Europe [55] and around the Faroe Islands [56,57]. Recent observations provide further support for cessation of Labrador Sea deep convection when negative salinity anomalies prevail east of the LC

realm and in the central convection region of the subpolar gyre [58]. Moreover, variations in Labrador Sea deep convection strongly control the spreading of dense Labrador Sea water masses at intermediate water depth of the North Atlantic, which also includes the deeper currents along the Greenland margin slope [59]. Furthermore, another study could confirm a relation between LC strength found to be at a maximum between 5.0 and 3.1 ka and circulation in the North Atlantic deep basin [60]. Complex, partly wind-driven interaction between northward advection of saline and warmer, southern-source surface water masses by the Gulfstream and North Atlantic Current (see Figure 1) and southward entrained low-salinity LC waters plays a further, important role in determining the strength of deep convection [61]. This water mass interaction is crucial with regard to subsurface warming and stratification of the subpolar North Atlantic, which has important implications for Greenland and Arctic glacier stability [62]. A fresher subpolar gyre around 4.2 ka with positive SST anomalies [54] in combination with an anomalously accelerated sea level rise [44] (p. 6) notably resembles very much the modern scenario linked to cessation of Labrador Sea deep convection [45] (p. 7). A weakening of the subpolar gyre and slowdown of the thermohaline circulation around 4.2 ka is thus concluded to signal a large-scale climate anomaly characterized by marked changes in ocean circulation in combination with more frequent atmospheric blocking. Additional evidence is provided by the reported blocking effects induced by a strengthened Siberian High [63]. A temporarily reduced ENSO variability with a dominant La Niña regime has been proposed to have prevailed during the 4.2 ka BP event [51], which is supported by actual climate research stating that Northern Hemisphere atmospheric blocking preferably occurs under La Niña conditions [64,65].

5. Conclusions

In southwest Greenland the late HTM resulted in widespread ice sheet melting in the period 4.4 to 3.2 ka, which is documented in marine sediment records from several fjords. The termination of this period with strong melt water outflow corresponds well with the reported timing of minimum GrIS extent at c. 3.0 ka. More prominent GrIS melt water pulses occurred between c. 4.4 ka and 4.0 ka, which appears to have led to an increased further freshening and cooling of LC surface waters off eastern Newfoundland. The latter melt water pulses coincided with an atmospheric warming peak and negative anomaly in the GrIS surface mass balance recorded in ice cores around 4.2 ka. In analogue to modern observations, enhanced ice sheet melting at that time may have been related to an atmospheric circulation regime characterized by Greenland blocking and associated increased northward transport of warm, Atlantic-derived water masses by the WGC. This period around 4.2 ka is well known for marked climate anomalies in many parts of the world (‘4.2 ka BP event’), and coincides with the internationally accepted boundary between Mid- and Late Holocene. Excessive melting in the southwest sector of the GrIS with associated increased melt water transport by the LC around 4.2 ka is concluded to have had a major impact on N-Atlantic Ocean subpolar gyre circulation which is supported by other studies that suggest a possible destabilization of the AMOC. We underline that complex atmosphere–ocean interaction processes must be taken into account here, in which, among others, the impact of strong GrIS melting on ocean circulation has played an important role.

Author Contributions: Conceptualization, A.K.; methodology, A.K. and M.-S.S.; A.K. and M.-S.S.; formal analysis, A.K. and M.-S.S.; investigation, A.K. and M.-S.S.; resources, A.K. and M.-S.S.; data curation, A.K. and M.-S.S.; writing—original draft preparation, A.K.; writing—review and editing, A.K. and M.-S.S.; visualization, A.K.; project administration, A.K. and M.-S.S.; funding acquisition, A.K. and M.-S.S. Our manuscript writing did not involve any supervising function. All authors have read and agreed to the published version of the manuscript.

Funding: By far most of the investigations involved would not have been possible without funding by the Independent Research Fund Denmark (DFF—Natural Sciences), with the most recent grant being the GreenFjords Project, grant no. 5241-00004B/FNU. Without listing all other funded projects, one exception worth mentioning was the NewGreen project, a joint contribution of above institutions to the International Polar Year, 2007. Ship-time on research vessels chartered for the sea-going work was in most cases likewise funded by DFF-Natural Sciences. Other agencies that occasionally had contributed in funding ship-time were the Mineral Resources Authority of Greenland, Nuuk, and the German Research Council (DFG), the latter having financially supported a cruise of RV Poseidon (1998) and RV "Alexander von Humboldt" (2002).

Data Availability Statement: Data are contained in the publications cited in Table 1 with each publication providing relevant repository information.

Acknowledgments: This review contribution is primarily based on the compilation and summary of a series of publi-cations resulting from a close scientific collaboration between the Geological Survey of Denmark and Greenland, Copenhagen, and the Institute of Geosciences, University of Aarhus, Denmark. Both institutions are sincerely acknowledged for their many years of facilitating these joint research efforts.

Conflicts of Interest: The authors declare no conflicts of interest. A.K. (presently emeritus) was employed by the Geological Survey of Denmark and Greenland. M.-S.S. (Aarhus University) declares that the research did not involve any commercial or financial relationship that could be interpreted as potential conflicts of interest. Both authors were funders of a large number of joint scientific projects (see Acknowledgements) and had participated in the design, the collection, analyses and interpretation of data published in many of the reported studies cited in this review article. The initiative for writing this article and first draft design have been the responsibility of the first author, while finalizing of the manuscript has been a joint effort with important input from the co-author.

References

1. Kaufman, D.S.; Ager, T.A.; Anderson, N.J.; Anderson, P.M.; Andrews, J.T.; Bartlein, P.J.; Brubaker, L.B.; Coats, L.L.; Cwynar, L.C.; Duvall, M.L.; et al. Holocene thermal maximum in the western Arctic (0–180° W). *Quat. Sci. Rev.* **2003**, *23*, 2059–2060. [CrossRef]
2. Axford, Y.; Losee, S.; Briner, J.P.; Francis, D.R.; Langdon, P.G.; Walker, I.R. Holocene temperature history at the western Greenland Ice Sheet margin reconstructed from lake sediments. *Quat. Sci. Rev.* **2013**, *59*, 87–100. [CrossRef]
3. Lecavalier, B.-S.; Fisher, D.A.; Milne, G.A.; Vinther, B.M.; Tarasov, L.; Huybrechts, P.; Lacerlle, D.; Main, B.; Zheng, J.; Bourgeois, J.; et al. High Arctic Holocene temperature record from the Agassiz ice cap and Greenland ice sheet evolution. *Proc. Natl. Acad. Sci. USA* **2017**, *114*, 5952–5957. [CrossRef] [PubMed]
4. Larsen, N.K.; Kjær, K.H.; Lecavalier, B.; Bjork, A.A.; Colding, S.; Huybrechts, P.; Jakobsen, K.E.; Kjeldsen, K.K.; Knudsen, K.-L.; Odgaard, B.V.; et al. The response of the southern Greenland ice sheet to the Holocene thermal maximum. *Geology* **2015**, *43*, 291–294. [CrossRef]
5. Levy, L.B.; Kelly, M.A.; Applegate, P.A.; Howley, J.A.; Virginia, R.A. Middle to late Holocene chronology of the western margin of the Greenland Ice Sheet: A comparison with Holocene temperature and precipitation records. *Arct. Antarct. Alp. Res.* **2018**, *18*, e1414477. [CrossRef]
6. Antwerpen, R.; Austermann, N.; Young, N.; Porter, D.; Lewright, L.; Latychev, K. Holocene southwest Greenland ice sheet behavior constrained by sea-level modeling. *Quat. Sci. Rev.* **2024**, *328*, 108553. [CrossRef]
7. Briner, J.P.; Kaufmann, D.S.; Bennike, O.; Kosnik, M.A. Amino acid ratios in reworked marine bivalve shells constrain Greenland Ice Sheet history during the Holocene. *Geology* **2014**, *42*, 75–78. [CrossRef]
8. Willemse, N.W.; Koster, E.A.; Hoogakker, B.; Van Tatenhove, F. A continuous record of Holocene eolian activity in West Greenland. *Quat. Res.* **2003**, *59*, 322–334. [CrossRef]
9. Andresen, C.S.; Björck, S.; Bennike, O.; Bond, G. Holocene climate changes in southern Greenland: Evidence from lake sediments. *J. Quat. Sci.* **2004**, *19*, 783–795. [CrossRef]
10. Krawczyk, D.W.; Batchelor, C.L.; Pearce, C.; Seidenkrantz, M.-S.; Sørensen, A.D.; Zinglersen, K.B. Stepwise deglaciation of the Nuup Kangerlua system, Southwest Greenland. *Cont. Shelf. Res.* **2026**, *300*, 105681. [CrossRef]
11. Westen, R.M.; Kliphuis, M.; Dijkstra, H.A. Collapse of the Atlantic Meridional Overturning Circulation in a Strongly Eddying Ocean-Only Model. *Geophys. Res. Lett.* **2025**, *52*, e2024GL114532. [CrossRef]
12. Caesar, L.; Rahmstorf, S.; Robinson, A.; Feulner, G.; Saba, V. Observed fingerprint of a weakening Atlantic Ocean overturning circulation. *Nature* **2018**, *556*, 191–196. [CrossRef] [PubMed]

13. Lloyd, J.M.; Kuijpers, A.; Long, A.; Moros, M.; Park, L.A. Foraminiferal reconstruction of mid-to late-Holocene ocean circulation and climate variability in Disko Bugt, West Greenland. *Holocene* **2007**, *17*, 1079–1091. [CrossRef]
14. Ren, J.; Jiang, H.; Seidenkrantz, M.-S.; Kuijpers, A. A diatom-based reconstruction of Early Holocene hydrographic and climatic change in a southwest Greenland fjord. *Mar. Micropaleontol.* **2009**, *70*, 166–176. [CrossRef]
15. Møller, H.S.; Jensen, K.G.; Kuijpers, A.; Aagaard-Sørensen, S. Late-Holocene environment and climatic changes in Ameralik Fjord, southwest Greenland: Evidence from the sedimentary record. *Holocene* **2006**, *16*, 685–695. [CrossRef]
16. Seidenkrantz, M.-S.; Aagaard-Sørensen, S.; Møller, H.S.; Kuijpers, A.; Jensen, K.G.; Kunzendorf, H. Hydrography and climatic change during the last 4400 years in Ameralik Fjord, SW Greenland. *Holocene* **2007**, *17*, 387–401. [CrossRef]
17. Lassen, S.J.; Kuijpers, A.; Kunzendorf, H.; Hoffmann-Wieck, G.; Mikkelsen, N.; Konradi, P. Late-Holocene Atlantic bottom-water variability in Igaliku Fjord, South Greenland, reconstructed fromforaminiferal faunas. *Holocene* **2004**, *14*, 165–171. [CrossRef]
18. Solignac, S.; Seidenkrantz, M.-S.; Jessen, C.; Kuijpers, A.; Gunvald, A.K.; Olsen, J. Late-Holocene sea-surface conditions offshore Newfoundland based on dinoflagellate cysts. *Holocene* **2011**, *21*, 539–552. [CrossRef]
19. Orme, L.C.; Miettinen, A.; Seidenkrantz, M.-S.; Tuominen, K.; Pearce, C.; Divine, D.V.; Oksman, M.; Kuijpers, A. Mid to late-Holocene sea-surface temperature variability off north-eastern Newfoundland and its linkage to the North Atlantic Oscillation. *Holocene* **2021**, *31*, 3–15. [CrossRef]
20. Cuny, J.; Rhines, P.B.; Niiler, P.P.; Bacon, S. Labrador Sea Boundary Currents and the Fate of the Irminger Sea Water. *J. Phys. Oceanogr.* **2002**, *32*, 627–647. [CrossRef]
21. Tang, C.C.L.; Ross, C.K.; Yao, T.; Petrie, B.; DeTracey, B.M.; Dunlap, E. The circulation, water masses and sea-ice of Baffin Bay. *Prog. Oceanogr.* **2004**, *63*, 183–228. [CrossRef]
22. Rysgaard, S.; Boone, W.; Carlson, D.; Sejr, M.K.; Bendtsen, J.; Juul-Pedersen, T.; Lund, H.; Meire, L.; Mortensen, J. An updated view on water masses on the pan-west Greenland continental shelf and their link to proglacial fjords. *J. Geophys. Res. Oceans* **2020**, *125*, e2019JC015564. [CrossRef]
23. Rignot, E.; Koppes, M.; Velicogna, I. Rapid submarine melting of the calving faces of West Greenland glaciers. *Nat. Geosci.* **2010**, *3*, 187–191. [CrossRef]
24. Azetsu-Scott, K.; Petrie, B.; Yeats, P.; Lee, C. Composition and fluxes of freshwater through Davis Strait using multiple chemical tracers. *J. Geophys. Res. Oceans* **2012**, *117*, C120111. [CrossRef]
25. Kuijpers, A.; Lloyd, J.M.; Jensen, J.B.; Endler, R.; Moros, M.; Park, L.A.; Schulz, B.; Jensen, K.G.; Laier, T. Late Quaternary circulation changes and sedimentation in Disko Bugt and adjacent fjords, central West Greenland. *Geol. Greenl. Surv. Bull.* **2001**, *189*, 41–47. [CrossRef]
26. Lloyd, J.M.; Park, L.A.; Kuijpers, A.; Moros, M. Early Holocene palaeoceanography and deglacial chronology of Disko Bugt, west Greenland. *Quat. Sci. Rev.* **2005**, *24*, 1741–1755. [CrossRef]
27. Erbs-Hansen, D.R.; Knudsen, K.L.; Olsen, J.; Lykke-Andersen, H.; Underbjerg, J.A.; Sha, L. Paleoceanographical development off Sisimiut, West Greenland, during the mid- end late Holocene. *Mar. Micropaleontol.* **2013**, *102*, 79–97. [CrossRef]
28. Kvorning, A.B.; Heikkilä, M.; Pearce, C.; Seidenkrantz, M.-S.; Simpson, G.L.; Meire, L.; Kuijpers, A.; Larsen, K.N.; Ribeiro, S. A Holocene fjord record from Greenland reveals exceptional Atlantic water influence during minimum ice-sheet extent. *Commun. Earth Environ.* **2025**, *6*, 326. [CrossRef]
29. Mortensen, J.; Lennert, K.; Bendtsen, J.; Rysgaard, S. Heat sources for glacial melt in a sub-Arctic fjord (Godthåbsfjord) in contact with the Greenland Ice Sheet. *J. Geophys. Res. Oceans* **2011**, *116*, 1–13. [CrossRef]
30. Overeem, I.; Hudson, B.D.; Syvitski, J.P.M.; Mikkelsen, A.B.; Hasholt, B.; Van den Broeke, M.R.; Noël, B.P.Y.; Morlighem, M. Substantial export of suspended sediment to the global oceans from glacial erosion in Greenland. *Nat. Geosci.* **2017**, *10*, 859–863. [CrossRef]
31. Andresen, C.S.; Karlsson, N.B.; Straneo, F.; Schmidt, S.; Andersen, T.J.; Eidam, E.F.; Bjørk, A.A.; Dartiguemalle, N.; Dyke, L.M.; Vermasssen, F.; et al. Sediment discharge from Greenland's marine-terminating glaciers is linked with surface melt. *Nat. Commun.* **2024**, *15*, 1332. [CrossRef] [PubMed]
32. Giraudeau, J.; Georgiades, E.; Caron, M.; Martinez, P.; St-Onge, G.; Billy, I.; Lebleu, P.; Ther, O.; Massé, G. A high-resolution elemental record of post-glacial lithic sedimentation in Upernavik Trough, western Greenland: History of ice-sheet dynamics and ocean circulation changes over the last 9100 years. *Glob. Planet. Change* **2020**, *191*, 103217. [CrossRef]
33. Stuart-Lee, A.E.; Mortensen, J.; Van der Kaaden, A.-S.; Meire, L. Seasonal Hydrography of Ameralik: A Southwest Greenland Fjord Impacted by a Land-Terminating Glacier. *J. Geophys. Res. Oceans* **2021**, *126*, e2021JC017552. [CrossRef]
34. Vinther, B.M.; Buchardt, S.L.; Clausen, H.B.; Dahl-Jensen, D.; Johnsen, S.J.; Fisher, D.A.; Koerner, R.M.; Raynaud, D.; Lipenkov, V.; Andersen, K.K.; et al. Holocene thinning of the Greenland ice sheet. *Nature* **2009**, *461*, 385–388. [CrossRef] [PubMed]
35. Gkinis, V.; Simonsen, S.B.; Buchardt, S.L.; White, J.W.C.; Vinther, B.M. Water isotope diffusion rates for the NorthGRIP ice core for the last 16,000 years—Glaciological and paleoclimatic implications. *Earth Planet. Sci. Lett.* **2014**, *405*, 132–141. [CrossRef]
36. Nielsen, L.T.; Adalgeirsdóttir, G.; Gkinis, V.; Nuterman, R.; Hvidberg, C.S. The effect of a Holocene climatic optimum on the evolution of the Greenland ice sheet during the last 10 kyr. *J. Glaciol.* **2018**, *64*, 477–488. [CrossRef]

37. Gao, Z.; Oliveira, R.; Feinberg, A.; Segato, D. Mercury accumulation over the Holocene from a Greenland ice core. *Sci. Adv.* **2026**, *12*, eaea0517. [CrossRef] [PubMed]
38. Dimento, B.P.; Mason, R.P.; Moore, C. The impact of sea ice on the air-sea exchange of mercury in the Arctic Ocean. *Deep. Sea Res. Part I Oceanogr. Res. Pap.* **2019**, *144*, 28–38. [CrossRef]
39. Weidick, A. Neoglacial change of ice cover and related response of the Earth's crust in West Greenland. *Grønl. Geol. Unders. Rap.* **1993**, *159*, 121–126. [CrossRef]
40. Allan, E.; de Vernal, A.; Seidenkrantz, M.-S.; Briner, J.P.; Hillaire-Marcel, C.; Pearce, C.; Meire, L.; Røy, H.; Mathiasen, A.M.; Nielsen, M.T.; et al. Insolation vs. meltwater control of productivity and sea surface conditions off SW Greenland during the Holocene. *Boreas* **2021**, *50*, 631–651. [CrossRef]
41. Larocca, L.J.; Axford, Y.; Bjørk, A.; Lasher, G.E.; Brooks, J.P. Local glaciers record delayed peak Holocene warmth in South Greenland. *Quat. Sci. Rev.* **2020**, *241*, 106421. [CrossRef]
42. Yang, Q.; Dixon, T.H.; Myers, P.G.; Bonin, J.; Chambers, D.; Van den Broeke, M.R. Recent increases in Arctic freshwater flux affects Labrador Sea convention and Atlantic overturning circulation. *Nat. Commun.* **2016**, *7*, 10525. [CrossRef] [PubMed]
43. Myers, P.G.; Castro de la Guardia, L.; Fu, C.; Gillard, L.C.; Grivault, N.; Hu, X.; Lee, C.M.; Moore, G.W.K.; Pennelly, C.; Ribergaard, M.H.; et al. Extreme High Greenland Blocking Index Leads to the Reversal of Davis and Nares Strait Net Transport Toward the Arctic Ocean. *Geophys. Res. Lett.* **2021**, *48*, e2021GL094178. [CrossRef]
44. Scott, D.B.; Collins, E.S. Late mid-Holocene sea-level oscillation: A possible cause. *Quat. Sci. Rev.* **1996**, *15*, 851–856. [CrossRef]
45. Yashyaev, I.; Zhang, Y. Concurrent warming, freshening and cessation of deep convection in the Labrador Sea raised its sea level to a record high. *Nat. Commun.* **2025**, *16*, 10721. [CrossRef] [PubMed]
46. Yashayev, I. Intensification and shutdown of deep convection in the Labrador Sea were caused by changes in atmospheric and freshwater dynamics. *Commun. Earth Environ.* **2024**, *5*, 156. [CrossRef]
47. Preece, J.R.; Mote, T.L.; Cohen, J.; Wachowicz, L.J.; Knox, J.A.; Tedesco, M.; Kooperman, G.J. Summer atmospheric circulation over Greenland in response to Arctic amplification and diminished spring snow cover. *Nat. Commun.* **2023**, *14*, 3759. [CrossRef] [PubMed]
48. Booth, R.K.; Jackson, S.T.; Forman, S.L.; Kutzbach, J.E.; Bettis, E.A.; Kreig, J.; Wright, D.K. A severe centennial-scale drought in mid-continental North America 4200 years ago and apparent global linkages. *Holocene* **2005**, *15*, 321–328. [CrossRef]
49. MacPherson, J.B. A 6 ka BP reconstruction for the Island of Newfoundland from the synthesis of Holocene lake-sediment pollen records. *Géographie Phys. Quat.* **1995**, *49*, 163–182.
50. Jessen, C.A.; Solignac, S.; Nørgaard-Pedersen, N.; Mikkelsen, N.; Kuijpers, A.; Seidenkrantz, M.-S. Exotic pollen as an indicator of variable atmospheric circulation over the Labrador Sea region during the mid to late Holocene. *J. Quat. Sci.* **2011**, *26*, 286–296. [CrossRef]
51. Weiss, H. Global megadrought, societal collapse and resilience at 4.2-3.9 ka BP across the Mediterranean and west Asia. *PAGES Mag.* **2016**, *24*, 61–63. [CrossRef]
52. Weiss, H.; Kuijpers, A.; Fisher, D.A. Global rearrangement of ocean-atmosphere interaction patterns forced Eastern Hemisphere societal collapses. In Proceedings of the EGU General Assembly 2023, Vienna, Austria, 23–28 April 2023. [CrossRef]
53. Klus, A.; Prange, M.; Varma, V.; Tremblay, L.B.; Schulz, M. Abrupt cold events in the North Atlantic Ocean in a transient Holocene simulation. *Clim. Past* **2018**, *14*, 1165–1178. [CrossRef]
54. Jalali, B.; Sicre, M.-A.; Azuara, J.; Pellichero, V.; Combourieu-Nebout, N. Influence of the North Atlantic subpolar gyre circulation on the 4.2 ka BP event. *Clim. Past* **2019**, *15*, 701–711. [CrossRef]
55. Earland, J.L.; Kender, S.; Schöne, B.; Sengupta, T.; Ward, S.L.; Bradley, S.L.; Blaauw, M.; Ascough, P.; Scourse, J.D. Asessing Atlantic subpolar gyre influence on the northern North Sea during the Holocene: A marine palaeoenvironmental reconstruction from the Fetlar basin (Shetland, UK). *Quat. Sci. Rev.* **2026**, *372*, 109711. [CrossRef]
56. Witon, E.; Malmgren, B.; Witkowski, A.; Kuijpers, A. Holocene marine diatoms from the Faeroe Islands and their paleoceanographic implications. *Palaeogeogr. Palaeoclimatol. Palaeoecol.* **2006**, *239*, 487–509. [CrossRef]
57. Staines-Urias, F.; Kuijpers, A.; Korte, C. Evolution of subpolar North Atlantic surface circulation since the early Holocene inferred from planktic foraminiferal and stable isotope records. *Quat. Sci. Rev.* **2013**, *76*, 66–81. [CrossRef]
58. Clement, C.; Frajka-Williams, E.; Von Oppeln-Bronikowski, N.; Goszczko, I.; de Young, B. Cessation of Labrador Sea Convection triggered by distinct fresh and warm (Sub)mesoscale Flows. *J. Phys. Oceanogr.* **2023**, *53*, 1959–1977. [CrossRef]
59. Böning, C.W.; Wagner, P.; Handmann, P.; Schwarzkopf, F.U.; Getzlaff, K.; Biastoch, A. Decadal changes in Atlantic overturning due to the excessive 1990's Labrador Sea convection. *Nat. Commun.* **2023**, *14*, 4635. [CrossRef] [PubMed]
60. Rashid, H.; Piper, D.J.W.; Lazar, K.B.; McDonald, K.; Saint-Ange, F. The Holocene Labrador Current: Changing linkages to atmospheric and oceanographic forcing factors. *Paleoceanogr. Paleoclimatology* **2017**, *32*, 498–510. [CrossRef]
61. Jutras, M.; Dufour, C.O.; Mucci, A.; Talbot, L.C. Large-scale control of the retroflection of the Labrador Current. *Nat. Commun.* **2023**, *14*, 2623. [CrossRef] [PubMed]

62. Menviel, L.C.; Pontes, G.; Lapeze, M.; Saini, H. Rapid subsurface warming in the subpolar North Atlantic from freshening. *Nat. Commun.* **2026**, *17*, 4653. [CrossRef] [PubMed]
63. Persoiu, A.; Ionita, M.; Weiss, H. Atmospheric blocking induced by the strengthened Siberian High led to drying in west Asia during the 4.2ka BP event—A hypothesis. *Clim. Past* **2019**, *15*, 781–793. [CrossRef]
64. Wiedemann, J.M.; Lupo, A.R.; Mokhov, I.I.; Tikhonova, E.A. The climatology of blocking anticyclones for the Northern and Southern Hemispheres: Block intensity as a diagnostic. *J. Clim.* **2002**, *15*, 3459–3473. [CrossRef]
65. Garcia-Burgos, M.; Gómara, I.; Rodríguez-Fonseca, B.; González-Alemán, J.J.; Zurita-Gotor, P.; Ayarzagüena, B. Abrupt and persisten atmospheric changes in the North Atlantic under La Nina conditions. *Weather Clim. Extrem.* **2023**, *42*, 100609. [CrossRef]

Disclaimer/Publisher's Note: The statements, opinions and data contained in all publications are solely those of the individual author(s) and contributor(s) and not of MDPI and/or the editor(s). MDPI and/or the editor(s) disclaim responsibility for any injury to people or property resulting from any ideas, methods, instructions or products referred to in the content.